



WILEY

ORIGINAL ARTICLE

Strontium-substituted biphasic calcium phosphate microspheres promoted degradation performance and enhanced bone regeneration

Ying Chen¹ | Zhongning Liu¹ | Ting Jiang¹ | Xinyu Zou² | Lei Lei¹ |
Wenjuan Yan³ | Jingwen Yang¹ | Bo Li²

¹Department of Prosthodontics, Peking University School and Hospital of Stomatology; National Clinical Research Center for Oral Diseases; National Engineering Laboratory for Digital and Material Technology of Stomatology; Beijing Key Laboratory of Digital Stomatology, Beijing, China

²Chongqing Key Laboratory of Nano/Micro Composite Materials and Devices, Chongqing University of Science and Technology, Chongqing, China

³First Clinical Division School and Hospital of Stomatology Peking University, Beijing, China

Correspondence

Ting Jiang, Department of Prosthodontics, Peking University School and Hospital of Stomatology; National Clinical Research Center for Oral Diseases; National Engineering Laboratory for Digital and Material Technology of Stomatology; Beijing Key Laboratory of Digital Stomatology, Beijing 100081, China. Email: jt_ketizu@163.com

Bo Li, Chongqing Key Laboratory of Nano/Micro Composite Materials and Devices, Chongqing University of Science and Technology, Chongqing 401331, China. Email: libo@cqust.edu.cn

Funding information

General Program of National Natural Science Foundation of China, Grant/Award Number: 81771045; Natural Science Foundation Project of CQ, Grant/Award Numbers: CSTC2016jcyjA0541, CSTC2018jcyjAX0711; Youth Program of National Natural Science Foundation of China, Grant/Award Number: 81400498

Abstract

Biphasic calcium phosphate (BCP) ceramics are the subject of much attention for use as bone replacement material. However, it remains a challenge to promote the degradation and osteoinductivity performances of BCP ceramics. In this work, novel BCP ceramic microspheres with good degradation and excellent osteoinductivity were prepared through high-content strontium (Sr) doping. The *in vitro* results indicated that the Sr10-BCP, Sr40-BCP, and Sr80-BCP microspheres all had their HA crystals partially transformed to the beta tricalcium phosphate phase following high-temperature sintering because of Ca-deficient HA formed by the partial substitution of Ca ions by Sr ions. In addition, the degradation rate was increased with the doping of increasing amounts of Sr. All prepared microspheres enhanced human bone marrow-derived mesenchymal stem cells attachment and proliferation. Specifically, among these modified microspheres, the Sr40-BCP microspheres showed the highest osteogenic potential. Furthermore, Sr40-BCP and HA microspheres were implanted in a calvarial defect model of rat to evaluate the *in vivo* bone augmentation ability. The results indicated that Sr40-BCP microspheres degraded more completely and significantly promoted new bone regeneration compared with HA microspheres. In conclusion, Sr40-BCP microspheres have excellent potential for degradation and bone regeneration and are promising osteogenic materials.

KEYWORDS

biphasic calcium phosphate, bone regeneration, degradation, microspheres, strontium-substituted

1 | INTRODUCTION

Biphasic calcium phosphate (BCP) ceramics, which are composed of poorly degradable hydroxyapatite (HA, $\text{Ca}_{10}(\text{PO}_4)_6(\text{OH})_2$) and

biodegradable beta tricalcium phosphate (β -TCP, β - $\text{Ca}_3(\text{PO}_4)_2$), have been considered to be promising bone replacement materials due to their good biocompatibility and osteoconductivity (Kim et al., 2012). Several studies have demonstrated that the osteoinductivity of BCP (Hong et al., 2010; Wang et al., 2014) is superior to that of pure HA (Yuan, van Blitterswijk, de Groot, & de Bruijn, 2006) or

Ying Chen and Zhongning Liu contributed equally to this study.

β -TCP (Kondo et al., 2006; Li et al., 2017). In general, BCP ceramics can be synthesized by physically mixing the pure HA and β -TCP or sintering calcium (Ca)-deficient apatite (Ca/P [phosphorus] < 1.67) at high temperature to chemically form a biphasic mixture (Vallet-Regí & González-Calbet, 2004). Compared with physically mixing, the chemical in situ synthesis possesses the advantages that the HA and β -TCP proportion can be regulated by controlling the Ca-deficient environment and that the HA and β -TCP phases in the resultant BCP can be mixed uniformly at atomic level. However, high temperature sintering in the process of chemical synthesis usually leads to a more perfect grain and poor degradation of BCP, thus reducing the biological activity (Fellah, Gauthier, Weiss, Chappard, & Layrolle, 2008; Yuan et al., 2010). Ideal biomaterials are expected to combine bioactive and degradable properties (Hench & Polak, 2002). Thus, it is important to improve the bioactivity and degradation of BCP ceramics. Previous studies have found that ions doping can cause lattice distortion and decrease crystallinity (He, Dong, & Deng, 2016), improving the degradation rate and biological response (Schumacher & Gelinsky, 2015).

Bone naturally contains some bioactive metal ions, such as magnesium (Mg), zinc (Zn), and strontium (Sr), which might be promising bioactive alternatives for ions doping. Furthermore, among these ions, Sr has drawn special attention due to its dual role in bone remodeling and biodegradation. For example, it can inhibit bone resorption by suppressing osteoclastic activity (Chung & Long, 2011; Peng et al., 2011) and promote bone regeneration by the Wnt/ β -catenin signaling pathway (Yang et al., 2011). Incorporation of Sr in HA ceramics can enhance degradability due to the replacement of Ca sites with Sr (Christoffersen, Christoffersen, Kolthoff, & Bärenholdt, 1997; Pan et al., 2009). Several in vitro studies suggested that Sr-substituted HA scaffolds promoted the osteogenic differentiation of human osteoblast-like cells (Li et al., 2017; Lin et al., 2013). However, BCP ceramics were not formed by these Sr-doped HA ceramics due to the absence of a β -TCP phase fraction. The degradation and osteogenic properties of such materials need to be optimized. Recently, several studies have focused on the effect of low-content Sr incorporation into HA on the β -TCP phase transformation, resulting in BCP ceramics (He et al., 2016; Nandha Kumar, Mishra, Udhay Kiran, & Kannan, 2015). In addition, a recent study has demonstrated that high content Sr incorporation into BCP ceramic enhanced its osteoinductivity (Deng et al., 2018). However, it has not been well studied that an appropriate high content of Sr incorporation into HA to induce a β -TCP phase transformation and improve the in vitro and in vivo performance of resultant BCP ceramics.

Herein, we describe the fabrication of high content Sr-doped BCP ceramic microspheres through the solid-in-oil-in-water (S/O/W) emulsion method. X-ray diffraction (XRD) was used to analyze the crystal structure and Sr occupied crystallographic sites of prepared microspheres. Then, the degradative and osteogenic performances of these novel materials were evaluated in vitro and in vivo. Thus, this work provides a novel Sr-substituted BCP microsphere system for various regenerative therapies.

2 | MATERIALS AND METHODS

2.1 | Materials

$\text{Sr}(\text{NO}_3)_2$, $\text{Ca}(\text{NO}_3)_2$, $(\text{NH}_4)_2\text{HPO}_4$, $\text{NH}_3 \cdot \text{H}_2\text{O}$, dichloromethane (DCM), polyvinyl butyral (PVB), and polyvinyl alcohol (PVA) were obtained from Sigma-Aldrich (St. Louis, MO).

2.2 | Preparation of Sr-BCP microspheres

Sr-HA powder was synthesized through a coprecipitated procedure. Briefly, $(\text{NH}_4)_2\text{HPO}_4$ solution (analytical grade, Aladdin) was dropwise added into a solution that containing $\text{Ca}(\text{NO}_3)_2$ and $\text{Sr}(\text{NO}_3)_2$ (both analytical grade, Aladdin) in the appropriate Ca/Sr molar ratios (10:0; 9:1; 6:4; 2:8) to acquire the (Sr + Ca)/P ratio of 1.67 (stoichiometric for HA). Meanwhile, the mixture was mechanical stirred at 400 rpm with a magnetic bar. To modify the pH to 10.0 ± 0.5 , ammonium hydroxide solution was applied during titration. The obtained precipitate was washed with deionized water for three times and then freeze dried at -60°C for 10 hr.

As shown in Figure 1a, the S/O/W emulsification method was adopted to prepare Sr-BCP microspheres, according to our previous report with modifications (Li, Liu, et al., 2017). The Sr-HA powder (10 wt%) was added to the oil phase comprising PVB (5 wt%) and DCM. After being mechanical stirred for 12 hr, the mixture was dropped into a water bath which containing 1 wt% PVA, and then stirred for 2 hr. These stabilized microspheres were freeze dried for 24 hr. A furnace was used to sinter the dried microspheres by heating to 600°C at a rate of $1^\circ\text{C}/\text{min}$ for 2 hr, then heating to $1,100^\circ\text{C}$ at a rate of $5^\circ\text{C}/\text{min}$ for another 2 hr. Finally, the furnace was naturally cooled to 25°C .

2.3 | Characterization of Sr-BCP and HA microspheres

The microstructure of these fabricated microspheres was evaluated by a scanning electron microscope (SEM, Hitachi S-4800, Japan). The phase composition of the prepared microspheres (Sr-BCP, HA) was characterized by XRD (X'pert Pro MPD, Philips) using Cu K α radiation in step-scan mode (2 hr = 0.02° per step). Elements (Ca, P, and Sr) concentrations of the microspheres were measured by X-ray spectroscopy (EDS) using Cu as a standard ($n = 5$).

2.4 | In vitro degradation behavior of Sr-BCP and HA microspheres

The dissolution reactions in vitro were initiated to evaluate the degradation property of ceramic microspheres and the degradation percentages were assessed by the released Ca ions concentration as shown in Figure S2. Briefly, Tris-HCl buffer (pH 7.4)

was used to immerse the microsphere samples at a concentration of 20 mg/ml in a thermostatic incubator at 37°C with the 200 rpm speed. A total of 50 μ l solution was extracted for test

and another 50 μ l fresh Tris-HCl buffer was added to it at every fixed time point. Finally, the absorbance of each sample was measured at 610 nm. The Ca content was calculated using the

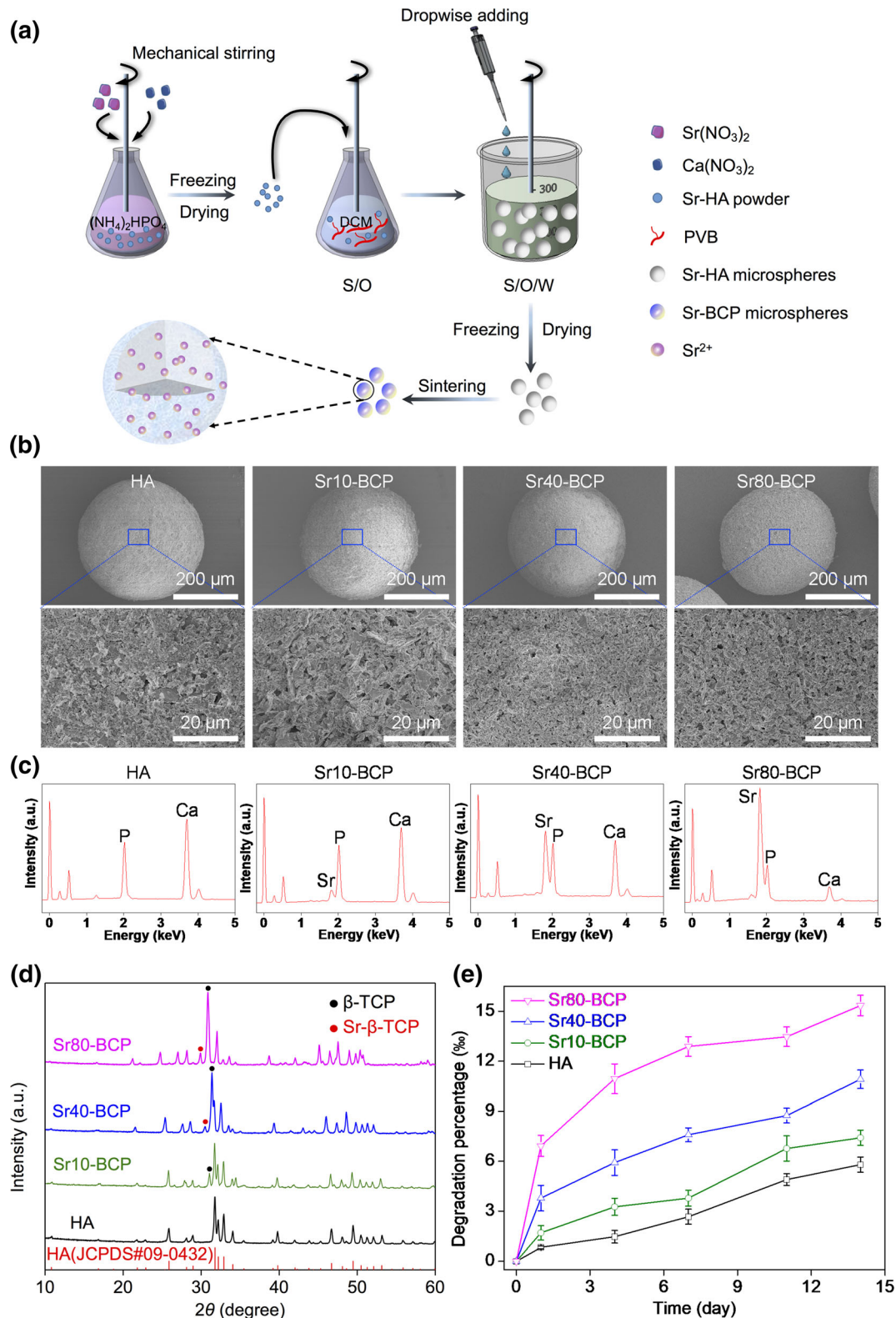


FIGURE 1 (a) Schematic of the fabrication of Sr-BCP microspheres via the S/O/W method, Sr was continuously dispersed in the Sr-BCP microspheres. (b) SEM micrographs and (c) corresponding EDS results of HA and Sr-BCP microspheres. (d) XRD patterns of HA and Sr-BCP microspheres. β -TCP phases were detected in all the synthetic Sr-BCP samples, Sr- β -TCP phases were found in Sr40-BCP and Sr80-BCP groups. (e) Degradation profiles in Tris-HCl buffer for HA and Sr-BCP microspheres

standard method provided in the kit (Jiangcheng Bioengineering Institute, Nanjing, China).

2.5 | In vitro studies

2.5.1 | Human bone marrow-derived mesenchymal stem cells (hBMSCs) morphology on microspheres

Sr-BCP and HA microspheres (5 mm³) were transferred to 24-well plates, respectively ($n = 3$), sterilized in 75% ethanol for 10 min. Then, 2×10^5 hBMSCs/well were seeded in 24-well plates, and cultured in alpha modification of Eagle's medium (α -MEM, Invitrogen, Waltham, MA) with 10% fetal bovine serum (FBS, Gibco, Gaithersburg, MD), 100 U/ml penicillin and 100 mg/ml streptomycin at 37°C in 5% CO₂.

Following hBMSCs cultured with microspheres for 24 hr, the samples were treated with 4% paraformaldehyde solution and washed with phosphonate buffered saline, then dehydrated through graded ethanol series. Finally, after freeze-drying overnight, all samples were sputtered with platinum, then observed using SEM.

To observe the morphology of cells on the microspheres, the cells seeded on microspheres were prepared as above, after being cultured for 24 hr, the samples were fixed by 4% paraformaldehyde solution. Then, they were treated with 0.1% triton X-100 and immersed in phalloidine (Cytoskeleton, PHDR1, America) for 30 min at 4°C in the dark. Next, they were mounted with DAPI (Beyotime, China), and a confocal microscope (ZEISS, LSM 710, Germany) was used to observe the morphology of cells on microspheres. Additionally, the numbers of hBMSCs attached on the surface of microspheres in five random fields were analyzed and calculated by using Image Pro Plus 6 software.

2.5.2 | Cell proliferation assay

Sr-BCP and HA microspheres extracts were prepared by adding 2 mg microspheres to 50 ml α -MEM medium. After soaking for 24 hr at 25°C, the extracts were collected. 5×10^3 cells/well were seeded in 96-well plates, microspheres (1 mm³) and their extracts were cocultured with the cells for 1–3 days, respectively. The cell counting kit-8 (CCK-8, Dojindo, Japan) assay was applied to determine the cytotoxicity of Sr-BCP and HA microspheres. The absorbance of the samples at 450 nm was measured by a spectrophotometer (Thermo).

2.5.3 | Alkaline phosphatase activity (ALP) test

Briefly, 2×10^5 ml⁻¹ cells were seeded in 24-well culture plates and cultured in α -MEM supplemented with 10% FBS for the first 24 hr. Then, the medium was replaced by Sr-BCP and HA microsphere extracts with 10% FBS and osteogenic differentiation medium (10 mM sodium b-glycerophosphate, 50 μ g/ml ascorbic acid, 100 nM dexamethasone). After 5 days, the cells were lysed in 1% Triton X-100 and collected by centrifugation for 15 min at 12,000 rpm. ALP activity was determined

with the ALP activity kit (Jiangcheng Bioengineering Institute, Nanjing, China) according to the manufacturer's instructions.

2.5.4 | Immunofluorescence staining of hBMSCs

2×10^5 hBMSCs were cocultured with Sr-BCP and HA microspheres (5 mm³) in 24-well plates for 24 hr in α -MEM supplemented with 10% FBS. Then, the basic culture medium was replaced by the osteogenic differentiation medium and the cells were osteoinductive cultured for 5 days. Immunofluorescence analysis was performed to assess the expression levels of osteogenic transcription factor osterix (OSX) in hBMSCs. Briefly, the cells were fixed with 4% paraformaldehyde for 30 min and treated with 0.5% Triton X-100 for 5 min. Then, the samples were incubated with primary antibody rabbit anti-OSX (Absin, China) and fluorescence secondary antibody. Finally, DAPI (Beyotime) was used to stain the nucleuses of hBMSCs. The cells were visualized by the confocal microscope immediately.

2.6 | In vivo assessment

2.6.1 | Critical-sized rat calvarial defect surgical procedure

The animals experiment procedures were approved by the Experimental Animal Care and Ethical Committee of Peking University (LA2017-155). Nine male Sprague Dawley (SD) rats were randomly divided into the following three groups: HA microspheres group ($n = 3$), Sr40-BCP microspheres group ($n = 3$), and control group (Ctrl) without material implanted ($n = 3$). The rats were anesthetized by 1% pentobarbital sodium, an approximately 2 cm incision was made, then the periosteum was bluntly dissected. A 5 mm electric trephine was employed to create two critical-sized defects on both sides of the cranial bone midline. The defects were then implanted with microspheres. The mucosa and skin incisions were sutured layer by layer.

2.6.2 | Microscopic computed tomography (micro-CT) assessment

Twelve weeks following the operation, all rats were euthanized, and the cranial bones were collected and fixed in 10% formalin. The collected calvaria were scanned using micro-CT (Siemens Inveon, Germany) with an X-ray source of 80 kV/500 μ A. The newly formed bone volume to total bone volume (BV/TV) in the defect area was calculated using Inveon Research Workplace.

2.6.3 | Bone histological analysis

The cranial bone was completely decalcified in 10% ethylenediaminetetraacetic acid (EDTA) for 8 weeks after micro-CT scanning.

All samples were dehydrated and then embedded in paraffin, and a microtome (Leika, Germany) was used to cut the samples of calvaria into 5 μm sections. Hematoxylin and eosin (H&E) and Masson staining were performed to enable examination of the new bone formation and materials in the defect. An osteogenesis marker, osteocalcin (OCN, Abcam, UK), was detected by immunohistochemical staining.

2.7 | Statistical analysis

The collected data are presented as the mean \pm SD. One-way analysis of variance (ANOVA) was used to analyze differences between groups. Statistical analyses were performed using SPSS v.10.1 software, * $p < .05$ was considered statistically significant.

3 | RESULTS

3.1 | Characterization of Sr-BCP microspheres

The HA and Sr-BCP microspheres were examined by SEM. As shown in Figure 1b, the composite spheres were successfully transformed into fine ceramic microspheres after being sintered at high temperature. The high magnification micrograph of corresponding samples showed that the surface of the microspheres was composed of micrometer grains. EDS spectra of microspheres illustrated the major peaks of Ca, P, and Sr elements, which showed that Sr ions were incorporated into HA in greater amounts (Figure 1c). The calculated Sr/(Ca + Sr) ratios and (Ca + Sr)/P ratios are listed in Table 1 and were close to the expected values.

The phase compositions of the control HA sample and synthetic Sr-BCP microspheres are shown in Figure 1d. Sr-BCP microspheres were confirmed to be fully apatitic. Compared with those in HA (JCPDS NO. 09-0432), the slight deviations in XRD peaks were attributed to Ca replacement by the larger ionic radius of Sr, which was judged by peak shift. Additionally, the crystallinity deteriorated with incorporation of Sr, as judged by peak broadening. Alternately, this may be due to the transformation of Ca-deficient apatite into HA, resulting in the detection of the β -TCP ($\text{Ca}_3(\text{PO}_4)_2$ JCPDS NO. 09-0169) phase in XRD. Moreover, with increasing Sr addition into the samples, Sr- β -TCP ($\text{Ca}_2\text{Sr}(\text{PO}_4)_2$ JCPDS NO. 52-0467) was formed in the Sr40-BCP and Sr80-BCP groups. To further evaluate the in vitro degradation performance of all the prepared samples, Ca

ions concentrations were determined in Tris-HCl buffer at fixed time points. The Ca ions concentration continued to increase from 0 to 14 days in the solution, which benefits bone formation (Figure S2). The trend of the degradation profiles was Sr80-BCP > Sr40-BCP > Sr10-BCP > HA (Figure 1e). These results indicate that the degradability of HA is enhanced by Sr incorporation and β -TCP phase transformation. Additionally, changing the HA/ β -TCP phase ratio can adjust the degradation properties.

3.2 | Morphology of hBMSCs on the microspheres

To confirm the biocompatibility and carrying capacity of microspheres with respect to hBMSCs, SEM images were obtained after coculturing with microspheres for 24 hr. The micrographs showed that filopodia of hBMSCs were extended and tightly adhered to the surface of Sr-BCP microspheres compared with HA microspheres (Figure 2a,b). Cell distributions were examined by fluorescent staining and confocal microscopy, and a greater number of cells were observed on Sr40-BCP microspheres than on other microspheres (Figure 2c-f).

3.3 | Effects of microspheres on hBMSCs in vitro

After hBMSCs were cultured with HA and Sr-BCP microspheres and their extracts for 1 and 3 days, CCK-8 assay results showed no significant differences in cell viability between the Sr-BCP and HA groups. However, there were significant differences between the microsphere stimulated groups (microspheres and their extracts) and non-microsphere stimulated (Ctrl) group (Figure 3a,b). Additionally, hBMSCs proliferated over time. These findings suggested that HA and Sr-BCP microspheres were noncytotoxic and could promote hBMSCs proliferation. As shown in Figure 3c, after osteogenesis induction culturing with microspheres extracts for 5 days, the ALP activity of the Sr40-BCP microspheres group was substantially higher than that of the other groups. Moreover, to evaluate the osteogenic response of hBMSCs on these microspheres, the cells were cocultured with microspheres and osteogenic inductive cultured for 5 days, the immunofluorescence staining findings indicated the OSX expression in Sr40-BCP microspheres group was remarkably stronger than that in other groups (Figure 3d-f). These results indicate that Sr40-BCP microspheres had a greater osteogenic effect.

3.4 | In vivo bone regeneration assessment

To evaluate the efficiency of microspheres in bone defect regeneration, cell-free Sr40-BCP microspheres and HA microspheres were implanted in a 5 mm calvarial bone defect; the same defect without any material implantation was applied as a control (Ctrl) group. Following implantation for 12 weeks, the harvested samples were scanned by micro-CT and then analyzed by histological observation. The micro-CT images showed that there was more newly formed

TABLE 1 The calculated Sr/(Ca + Sr) and (Ca + Sr)/P ratios of the synthetic HA and Sr-BCP microspheres (mean \pm SD, $n = 5$)

Sample	Sr/(Ca + Sr) mol % In sol	Sr/(Ca + Sr) mol % In product	(Ca + Sr)/P In product
HA	0	0	1.54 \pm 0.02
Sr10-BCP	10	8.97 \pm 0.21	1.57 \pm 0.03
Sr40-BCP	40	37.99 \pm 0.53	1.63 \pm 0.04
Sr80-BCP	80	79.37 \pm 0.65	1.81 \pm 0.04

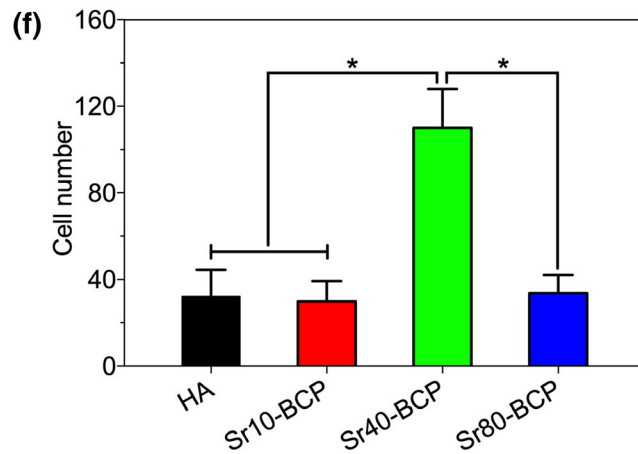
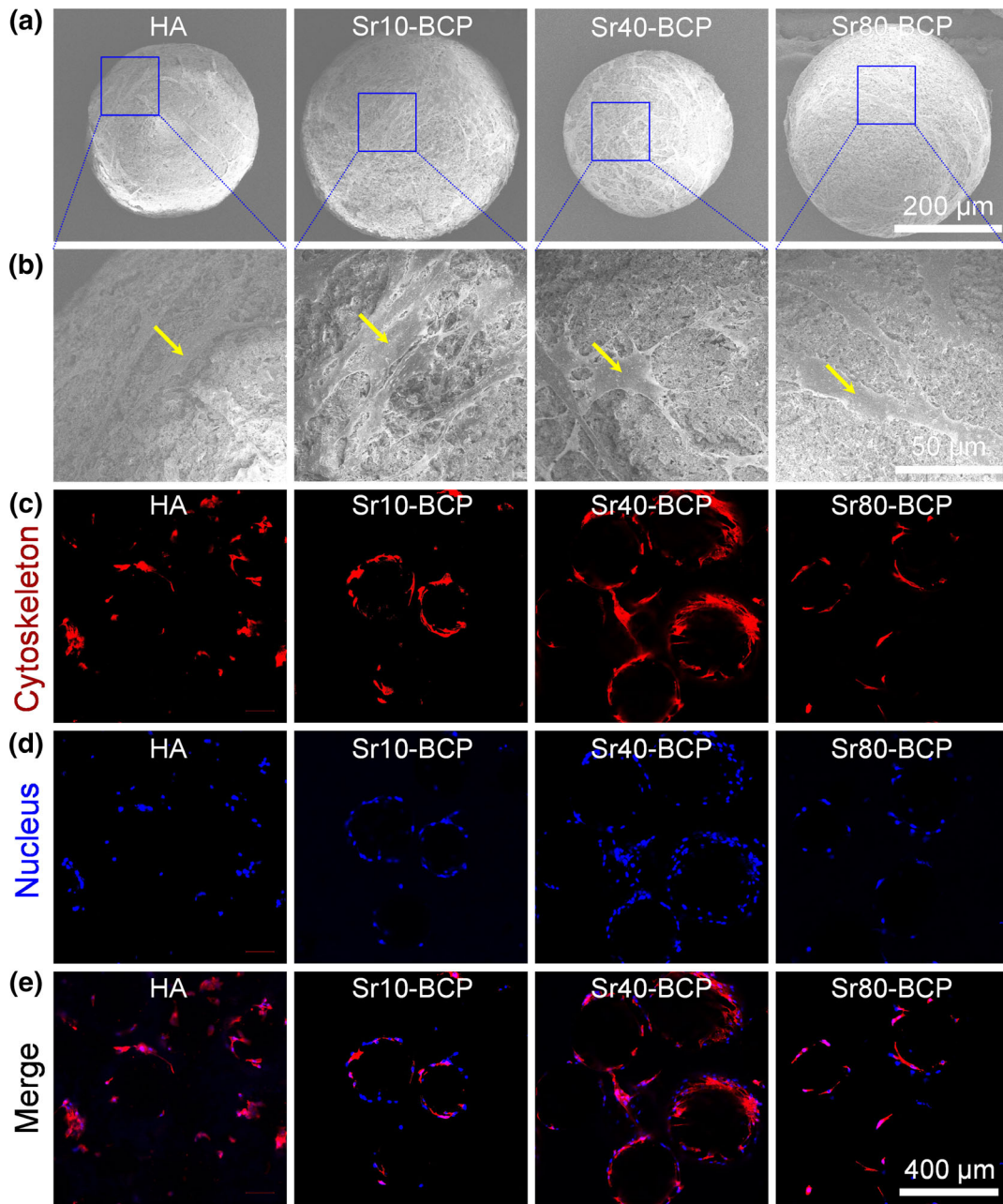


FIGURE 2 Legend on next page.

bone in the bone defect area in the Sr40-BCP microspheres group compared with that in the Ctrl and HA groups. Moreover, most of the Sr40-BCP microspheres were degraded relative to the HA microspheres group (Figure 4a). The proportion of newly formed bone tissue (BV/TV) in the Sr40-BCP group was significantly higher than that in the Ctrl and HA groups (Figure 4b). To further evaluate the newly formed bone structure, the collected samples were stained with H&E, Masson, and OCN. H&E and Masson staining showed that in the Sr40-BCP microspheres group, a substantial amount of new bone formed at the edge of defect, microspheres which typically remain were scarcely observed. However, the defects treated with HA microspheres were mainly filled with fibrous tissue and a large amount of nondegraded HA microspheres, with limited new bone formation (Figure 4c). The Masson staining results were consistent with H&E staining, with abundant collagen fibers and new bone formation in the Sr40-BCP group (Figure 4d). Moreover, the osteogenic activity of these microspheres was further analyzed by OCN immunohistochemical staining. As shown in Figure 4e, the Sr40-BCP microsphere group demonstrated stronger expression of OCN than the other two groups.

4 | DISCUSSION

Among the CaP ceramics, synthetic HA has been used as a scaffold to repair bone defects due to its highly biomimetic chemical formula and properties. However, poor degradability hinders its clinical application (Böhner et al., 2005). β -TCP with a lower Ca/P ratio of 1.5 possesses better degradability than HA and has been extensively studied for bone regeneration. However, it remains a challenge to maintain the needed mechanical support during the initial stage of implantation and to avoid detrimental effects on surrounding newly formed bone tissues due to rapid degradation at longer times (Yuan et al., 2001). In addition, improvement in maturity of new bone formed by β -TCP is needed as our previous study demonstrated (Li, Liu, et al., 2017). Therefore, BCP ceramic, a composite mixture of HA and β -TCP, has been developed to overcome the weaknesses of pure HA and β -TCP. Moreover, it has been proven that the potential of osteoinductivity is $\text{BCP} > \beta\text{-TCP} > \text{HA}$ (Samavedi, Whittington, & Goldstein, 2013), which is affected by material characteristics including ionic environment, phase composition, degradation, and structure (Tang, Li, Tan, Fan, & Zhang, 2018). In order to further improve the degradation and osteoinductivity of BCP, Sr-substituted BCP holds promise in promoting these properties.

In this work, different Sr concentration-substituted BCP microspheres were prepared using the chemical synthesis method, and the β -TCP phase transformation was assessed. The XRD results demonstrate that all the Sr-doped HA ceramics (Sr10-BCP, Sr40-BCP, and Sr80-BCP) had β -TCP phase transformed following exposure to high

temperatures, and β -TCP was increased with the incorporation of increasing amounts of Sr ions. Moreover, another phase (Sr- β -TCP) was formed in both Sr40-BCP and Sr80-BCP groups (Figure 1d). The mechanism behind this phenomenon can be explained as follows: during the preparation of Sr-BCP powder as starting materials, it produced some Ca-deficient HA ($\text{Ca}_x\text{Sr}_{10-x}(\text{PO}_4)_6(\text{OH})_2$) powder because of the substitution of Sr for Ca, which weakened the integrity of HA lattice. Following exposure to high temperature during sintering, the Ca-deficient HA was decomposed into β -TCP and HA (Raynaud, Champion, Bernache-Assollant, & Thomas, 2002), thereby resulting in Sr-BCP microspheres. The addition of low levels of Sr did not affect the crystallinity and stability of HA greatly. However, as Sr content increased, more Ca-deficient HA was produced, and more Sr ions tended to become inserted into β -TCP to form Sr- β -TCP. It has been reported that Sr ions preferentially occupy the Ca 4 site of β -TCP and increase the stability of the β -TCP structure (Renaudin, Laquerrière, Filinchuk, Jallot, & Nedelec, 2008).

It is well accepted that a reasonable rate of scaffold degradation is extremely important in bone tissue engineering, which contributes to new bone tissue ingrowth and favorable integration with surrounding native bone. HA is the least soluble among CaP ceramics because of its high Ca/P molar ratio. It has great potential to host various ions in its crystal lattice to improve its degradation. In our study, the lattice of HA was changed, and the degradation performance was improved by adding strontium. In addition, the degradation performance was further improved by β -TCP produced by high temperature sintering, and the degradation rate could be adjusted by adjusting the HA/ β -TCP ratio (Figure 1e). However, it remains an inherent challenge for degradable ceramics that the high concentration release of metal ions (Ca, Sr, and P) may have a detrimental effect on surrounding tissues. Therefore, it was vital to evaluate the toxicity of all the resulting microspheres. As seen from the SEM, fluorescent staining of cytoskeleton, and CCK-8 results, both HA and Sr-BCP microspheres were non-cytotoxic and beneficial for cell proliferation. Moreover, Sr40-BCP microspheres possessed an excellent cell carrying capacity (Figure 2f).

The aim of our study was to determine the effect of Sr addition on the degradation of HA and further develop an ideal microsphere scaffold with osteogenic and biodegradable capacities. Hence, the osteogenic differentiation effect was evaluated by ALP activity and immunofluorescence staining of OSX in hBMSCs. The upregulation of ALP is a pivotal event in early osteogenesis, which participates in mineralization (Gaharwar et al., 2013; Wang et al., 2007). OSX is also a marker of osteogenesis, which promotes osteoblast differentiation (Chen, Song, Yang, Huang, & Jiang, 2019). The higher levels of ALP and OSX expression in Sr40-BCP group both indicated the promotion effect of Sr40-BCP microspheres on osteogenesis. This might be due to the different concentration of ions (Ca, P, and Sr) release from the

FIGURE 2 (a, b) SEM micrographs of hBMSCs seeding on HA and Sr-BCP microspheres. Arrows were placed for cells, and filopodia of hBMSCs were extended and tightly adhered to the surface of Sr-BCP microspheres. (c–e) Fluorescent staining and confocal images of cells seeded on HA and Sr-BCP microspheres. The cytoskeleton was stained red by phalloidine (c), and the nucleus was stained blue by DAPI (d). (e) The merged images of cytoskeleton and nucleus, hBMSCs fully covered and adhered to Sr40-BCP microspheres. (f) The calculated numbers of hBMSCs attached on the surface of microspheres, and more cells were attached on the surface of Sr40-BCP microspheres. $n = 5$, $*p < .05$

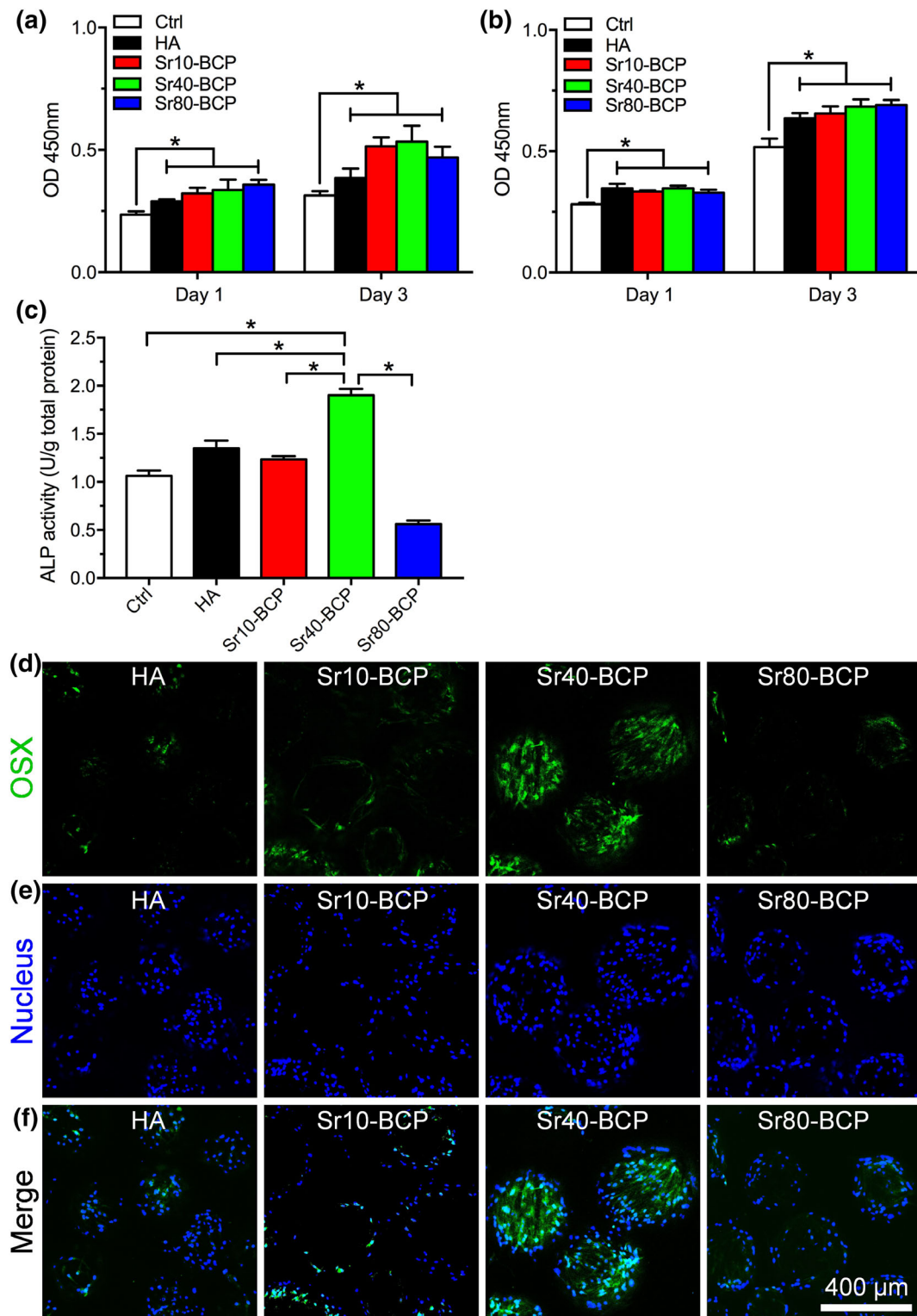
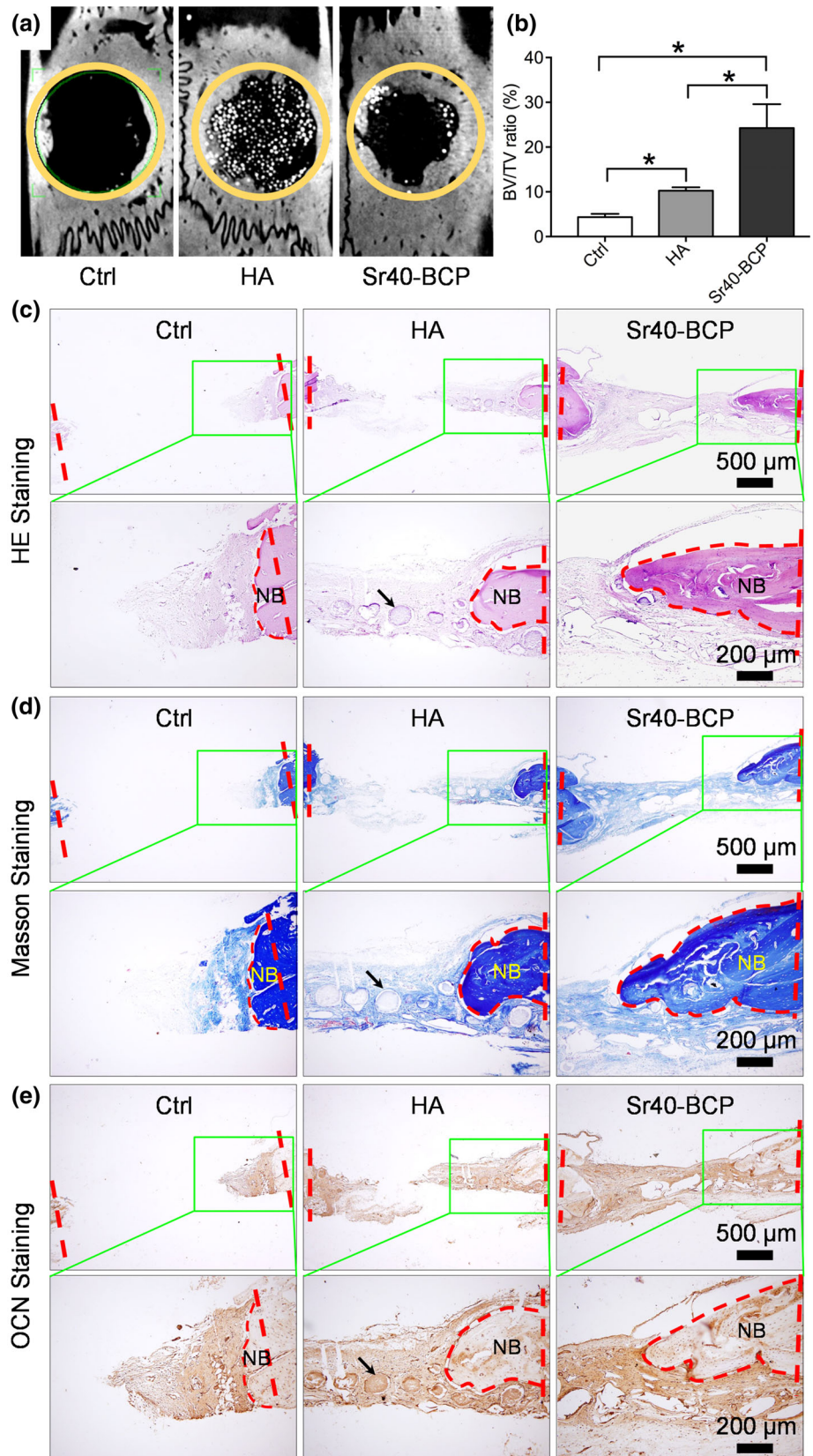


FIGURE 3 Cell viability measured using the CCK-8 assay of hBMSCs cultured with HA and Sr-BCP microspheres (a) and their extracts (b) for 1 and 3 days. (c) ALP activity of hBMSCs treated with HA and Sr-BCP microsphere extracts 5 days after induction of osteogenesis. (d) Immunostaining images of osteogenic related marker OSX (green) and (e) the nucleus of hBMSCs cultured with microspheres for 5 days following osteogenic induction. (f) The merged images of OSX and nucleus, a remarkably higher expression of OSX in Sr40-BCP group than other groups. The Sr40-BCP group showed an excellent osteogenesis effect. $n = 3$, $*p < .05$

Sr-BCP. Previous studies showed that a certain concentration of Ca and P ions released from Ca-P ceramics could promote the osteogenic differentiation of BMSCs (Barradas et al., 2012; Tang et al., 2017).

Moreover, Sr plays a synergistic role in osteogenesis by suppressing osteoclast differentiation and promoting osteoblast proliferation and differentiation (Peng et al., 2011; Yang et al., 2011). However, these

FIGURE 4 In vivo evaluation of bone regeneration in each group. (a) Micro-CT images of bone regeneration. (b) Proportion of mineralized tissue (BV/TV) in the defects implanted with microspheres. (c) H&E staining of acquired cranial bone to observe the newly formed bone and microspheres remaining. (d) Masson trichrome staining for collagen fibers in the defects. (e) OCN immunohistochemical staining for osteogenic activity. NB refers to newly formed bone. Arrows indicate undegraded materials



functions of Sr are strongly dose dependent. In instance, low levels (1–3 mmol/L) of Sr exerted promoting effects on the proliferation and osteogenic differentiation of BMSCs (Peng et al., 2009). High concentration of Sr (>5 mmol/L) inhibited the proliferation and osteogenic

differentiation of BMSCs markedly (Schumacher, Lode, Helth, & Gelinsky, 2013). Hence, different concentrations of Sr substituted BCP microspheres endowed different release concentration of Sr, and the Sr40 was a proper concentration for osteogenic differentiation. After

implantation, Sr40-BCP microspheres provided a cache of mineral ions (Ca, P, and Sr). Moreover, the transformation from the Ca-deficient HA to the β -TCP phase and partial Ca substitution by Sr enhanced the degradation property of Sr-BCP microspheres, which provided more mineral ions. It was seen that the *in vivo* bone regeneration capacity of Sr40-BCP microspheres was superior to that of HA microspheres and there were fewer Sr40-BCP microspheres remaining than HA microspheres. These results are probably due to the β -TCP and sustained release of Sr at an appropriate dosage; there is an interaction between the two, and a balance must be reached; here, 40% Sr-doped HA appears to strike that balance.

In summary, the strategy of adding Sr to HA for superior degradation was proven to be possible. This study demonstrates that 40% Sr-doping is an ideal concentration, which reached a balance between reasonable degradation and new bone formation.

5 | CONCLUSIONS

In this study, we fabricated the novel Sr-BCP microspheres by a simple S/O/W emulsion procedure, and they possessed a better hBMSC loading capacity than HA microspheres. Moreover, our results demonstrate the dual effect of high content Sr doping on improving the degradation and osteogenesis performances of BCP ceramics. Meanwhile, Sr40-BCP microspheres met an ideal balance between a reasonable degradation rate and bone formation. Our findings shed light on enhancing the degradation of BCP ceramics to match the rate of new bone formation, thus promoting bone regeneration.

ACKNOWLEDGMENTS

Funding for this work was supported by Youth Program of National Natural Science Foundation of China (Grant No. 81400498); the General Program of National Natural Science Foundation of China (Grant No.81771045); and the Natural Science Foundation Project of CQ (Grant No. CSTC2016jcyjA0541, CSTC2018jcyjAX0711).

CONFLICT OF INTEREST

The authors declare no competing interests.

REFERENCES

- Barradas, A. M. C., Fernandes, H. A. M., Groen, N., Chai, Y. C., Schrooten, J., van de Peppel, J., ... de Boer, J. (2012). A calcium-induced signaling cascade leading to osteogenic differentiation of human bone marrow-derived mesenchymal stromal cells. *Biomaterials*, 33(11), 3205–3215.
- Bohner, M., van Lenthe, G. H., Grünenfelder, S., Hirsiger, W., Evison, R., & Müller, R. (2005). Synthesis and characterization of porous β -tricalcium phosphate blocks. *Biomaterials*, 26(31), 6099–6105.
- Chen, Z., Song, Z., Yang, J., Huang, J., & Jiang, H. (2019). Sp7/osterix positively regulates *dlx2b* and *bglap* to affect tooth development and bone mineralization in zebrafish larvae. *Journal of Biosciences*, 44(6), 127.
- Christoffersen, J., Christoffersen, M. R., Kolthoff, N., & Bärenholdt, O. (1997). Effects of strontium ions on growth and dissolution of hydroxyapatite and on bone mineral detection. *Bone*, 20(1), 47–54.
- Chung, C.-J., & Long, H.-Y. (2011). Systematic strontium substitution in hydroxyapatite coatings on titanium via micro-arc treatment and their osteoblast/osteoclast responses. *Acta Biomaterialia*, 7(11), 4081–4087.
- Deng, Y., Liu, M., Chen, X., Wang, M., Li, X., Xiao, Y., & Zhang, X. (2018). Enhanced osteoinductivity of porous biphasic calcium phosphate ceramic beads with high content of strontium-incorporated calcium-deficient hydroxyapatite. *Journal of Materials Chemistry B*, 6(41), 6572–6584.
- Fellah, B. H., Gauthier, O., Weiss, P., Chappard, D., & Layrolle, P. (2008). Osteogenicity of biphasic calcium phosphate ceramics and bone autograft in a goat model. *Biomaterials*, 29(9), 1177–1188.
- Gaharwar, A. K., Mihaila, S. M., Swami, A., Patel, A., Sant, S., Reis, R. L., ... Khademhosseini, A. (2013). Bioactive silicate nanoplatelets for osteogenic differentiation of human mesenchymal stem cells. *Advanced Materials*, 25(24), 3329–3336.
- He, L., Dong, G., & Deng, C. (2016). Effects of strontium substitution on the phase transformation and crystal structure of calcium phosphate derived by chemical precipitation. *Ceramics International*, 42(10), 11918–11923.
- Hench, L. L., & Polak, J. M. (2002). Third-generation biomedical materials. *Science*, 295(5557), 1014–1017.
- Hong, Y., Fan, H., Li, B., Guo, B., Liu, M., & Zhang, X. (2010). Fabrication, biological effects, and medical applications of calcium phosphate nanoceramics. *Materials Science and Engineering R*, 70(3), 225–242.
- Kim, T.-W., Lee, H.-S., Kim, D.-H., Jin, H.-H., Hwang, K.-H., Lee, J. K., ... Yoon, S.-Y. (2012). *In situ* synthesis of magnesium-substituted biphasic calcium phosphate and *in vitro* biodegradation. *Materials Research Bulletin*, 47(9), 2506–2512.
- Kondo, N., Ogose, A., Tokunaga, K., Umezumi, H., Arai, K., Kudo, N., ... Endo, N. (2006). Osteoinduction with highly purified β -tricalcium phosphate in dog dorsal muscles and the proliferation of osteoclasts before heterotopic bone formation. *Biomaterials*, 27(25), 4419–4427.
- Li, B., Liu, Z., Yang, J., Yi, Z., Xiao, W., Liu, X., ... Liao, X. (2017). Preparation of bioactive β -tricalcium phosphate microspheres as bone graft substitute materials. *Materials Science and Engineering: C*, 70(Pt 2), 1200–1205.
- Li, J., Yang, L., Guo, X., Cui, W., Yang, S., Wang, J., ... Xu, S. (2017). Osteogenesis effects of strontium-substituted hydroxyapatite coatings on true bone ceramic surfaces *in vitro* and *in vivo*. *Biomedical Materials*, 13(1), 015018.
- Lin, K., Liu, P., Wei, L., Zou, Z., Zhang, W., Qian, Y., ... Chang, J. (2013). Strontium substituted hydroxyapatite porous microspheres: surfactant-free hydrothermal synthesis, enhanced biological response and sustained drug release. *Chemical Engineering Journal*, 222, 49–59.
- Nandha Kumar, P., Mishra, S. K., Udhay Kiran, R., & Kannan, S. (2015). Preferential occupancy of strontium in the hydroxyapatite lattice in biphasic mixtures formed from non-stoichiometric calcium apatites. *Dalton Transactions*, 44(17), 8284–8292.
- Pan, H. B., Li, Z. Y., Lam, W. M., Wong, J. C., Darvell, B. W., Luk, K. D. K., & Lu, W. W. (2009). Solubility of strontium-substituted apatite by solid titration. *Acta Biomaterialia*, 5(5), 1678–1685.
- Peng, S., Liu, X. S., Huang, S., Li, Z., Pan, H., Zhen, W., ... Lu, W. W. (2011). The cross-talk between osteoclasts and osteoblasts in response to strontium treatment: involvement of osteoprotegerin. *Bone*, 49(6), 1290–1298.
- Peng, S., Zhou, G., Luk, K. D. K., Cheung, K. M. C., Li, Z., Lam, W. M., ... Lu, W. W. (2009). Strontium promotes osteogenic differentiation of mesenchymal stem cells through the Ras/MAPK signaling pathway. *Cellular Physiology and Biochemistry*, 23(1–3), 165–174.
- Raynaud, S., Champion, E., Bernache-Assollant, D., & Thomas, P. (2002). Calcium phosphate apatites with variable Ca/P atomic ratio I. Synthesis, characterisation and thermal stability of powders. *Biomaterials*, 23(4), 1065–1072.

- Renaudin, G., Laquerrière, P., Filinchuk, Y., Jallot, E., & Nedelec, J. M. (2008). Structural characterization of sol-gel derived Sr-substituted calcium phosphates with anti-osteoporotic and anti-inflammatory properties. *Journal of Materials Chemistry*, 18(30), 3593–3600.
- Samavedi, S., Whittington, A. R., & Goldstein, A. S. (2013). Calcium phosphate ceramics in bone tissue engineering: A review of properties and their influence on cell behavior. *Acta Biomaterialia*, 9(9), 8037–8045.
- Schumacher, M., & Gelinsky, M. (2015). Strontium modified calcium phosphate cements - approaches towards targeted stimulation of bone turnover. *Journal of Materials Chemistry B*, 3(23), 4626–4640.
- Schumacher, M., Lode, A., Helth, A., & Gelinsky, M. (2013). A novel strontium(II)-modified calcium phosphate bone cement stimulates human-bone-marrow-derived mesenchymal stem cell proliferation and osteogenic differentiation *in vitro*. *Acta Biomaterialia*, 9(12), 9547–9557.
- Tang, Z., Li, X., Tan, Y., Fan, H., & Zhang, X. (2018). The material and biological characteristics of osteoinductive calcium phosphate ceramics. *Regenerative Biomaterials*, 5(1), 43–59.
- Tang, Z., Tan, Y., Ni, Y., Wang, J., Zhu, X., Fan, Y., ... Zhang, X. (2017). Comparison of ectopic bone formation process induced by four calcium phosphate ceramics in mice. *Materials Science and Engineering: C*, 70 (Pt2), 1000–1010.
- Vallet-Regí, M., & González-Calbet, J. M. (2004). Calcium phosphates as substitution of bone tissues. *Progress in Solid State Chemistry*, 32 (1), 1–31.
- Wang, J., Chen, Y., Zhu, X., Yuan, T., Tan, Y., Fan, Y., & Zhang, X. (2014). Effect of phase composition on protein adsorption and osteoinduction of porous calcium phosphate ceramics in mice. *Journal of Biomedical Materials Research. Part A*, 102(12), 4234–4243.
- Wang, Y., Zhang, S., Zeng, X., Ma, L. L., Weng, W., Yan, W., & Qian, M. (2007). Osteoblastic cell response on fluoridated hydroxyapatite coatings. *Acta Biomaterialia*, 3(2), 191–197.
- Yang, F., Yang, D., Tu, J., Zheng, Q., Cai, L., & Wang, L. (2011). Strontium enhances osteogenic differentiation of mesenchymal stem cells and *in vivo* bone formation by activating Wnt/catenin signaling. *Stem Cells*, 29(6), 981–991.
- Yuan, H., Bruijn, J. D. D., Li, Y., Feng, J., Yang, Z., Groot, K. D., & Zhang, X. (2001). Bone formation induced by calcium phosphate ceramics in soft tissue of dogs: a comparative study between porous α -TCP and β -TCP. *Journal of Materials Science: Materials in Medicine*, 12(1), 7–13.
- Yuan, H., Fernandes, H., Habibovic, P., de Boer, J., Barradas, A. M. C., de Rooter, A., ... de Bruijn, J. D. (2010). Osteoinductive ceramics as a synthetic alternative to autologous bone grafting. *Proceedings of the National Academy of Sciences of the United States of America*, 107(31), 13614–13619.
- Yuan, H., van Blitterswijk, C. A., de Groot, K., & de Bruijn, J. D. (2006). A comparison of bone formation in biphasic calcium phosphate (BCP) and hydroxyapatite (HA) implanted in muscle and bone of dogs at different time periods. *Journal of Biomedical Materials Research. Part A*, 78(1), 139–147.

SUPPORTING INFORMATION

Additional supporting information may be found online in the Supporting Information section at the end of this article.

How to cite this article: Chen Y, Liu Z, Jiang T, et al. Strontium-substituted biphasic calcium phosphate microspheres promoted degradation performance and enhanced bone regeneration. *J Biomed Mater Res*. 2020;108: 895–905. <https://doi.org/10.1002/jbm.a.36867>